

Electronic Supplementary Information

Single lithium-ion conducting monomer as a SEI-forming additive for lithium-ion batteries

Jin-Hong Seok^a, Seongjae Lee^a, Da-Ae Lim^a, Kyoung Ho Ahn^b, Chul Haeng Lee^b, Kyeounghak Kim^a and Dong-Won Kim^{*a}

^aDepartment of Chemical Engineering, Hanyang University, Seoul 04763, Republic of Korea

^bBattery R&D, LG Energy Solution, Ltd, Daejeon 34122, Republic of Korea

* Corresponding author: dongwonkim@hanyang.ac.kr.

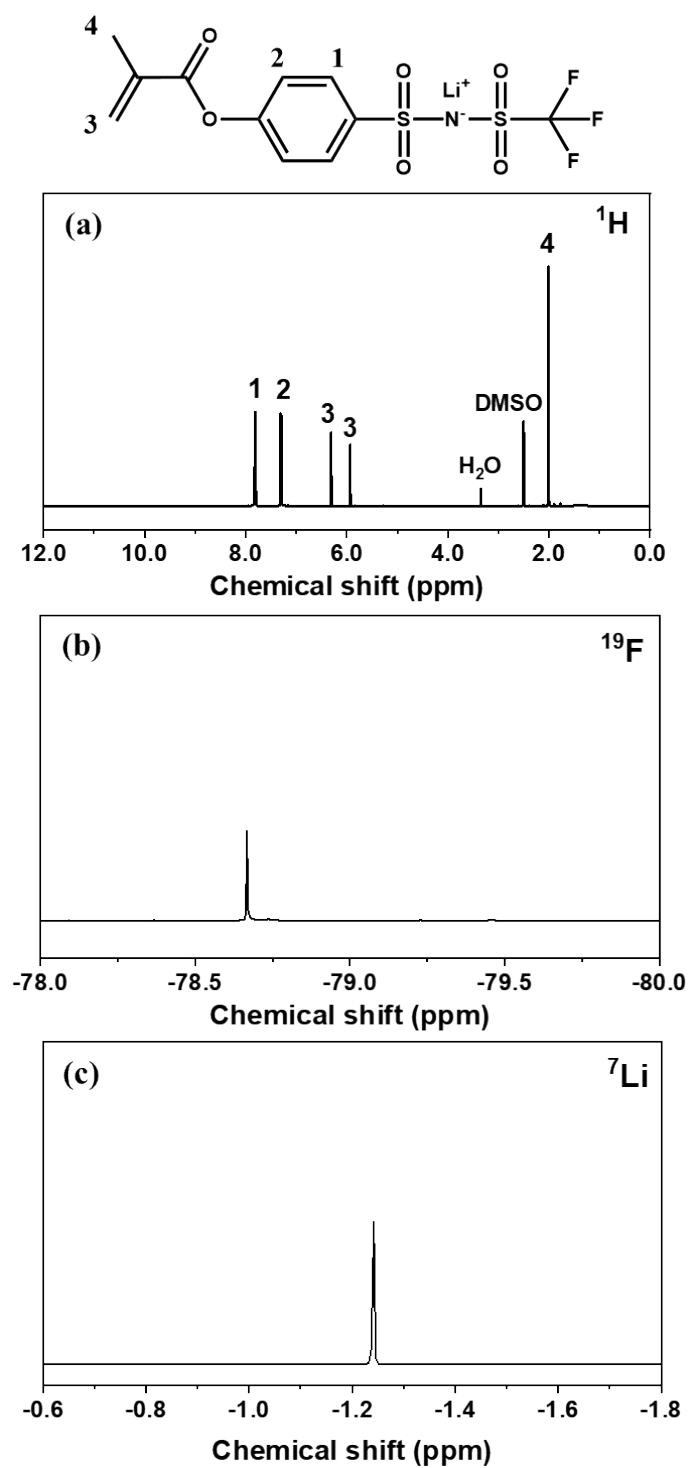


Fig. S1. (a) ^1H , (b) ^{19}F and (c) ^7Li NMR spectra of LiMPTFSI.

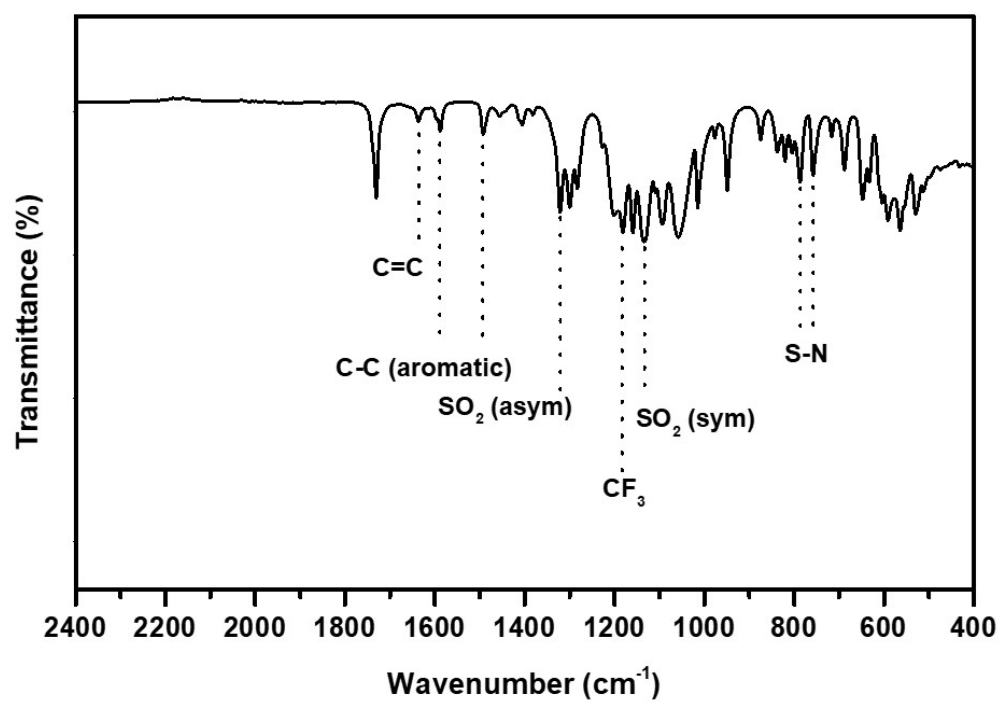


Fig. S2. FT-IR spectrum of LiMPTFSI.

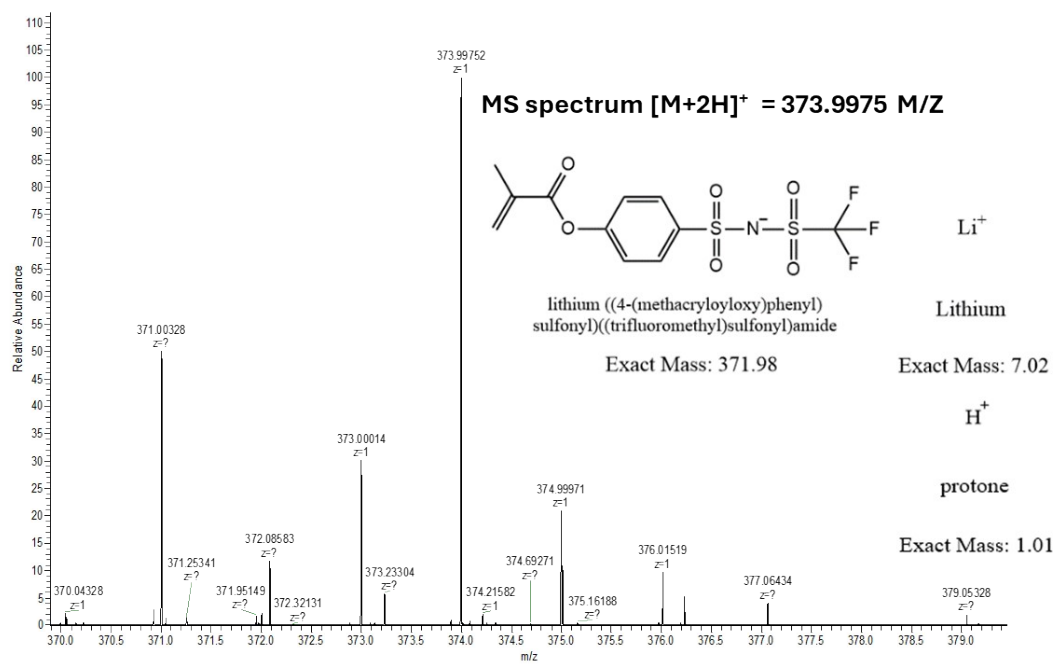
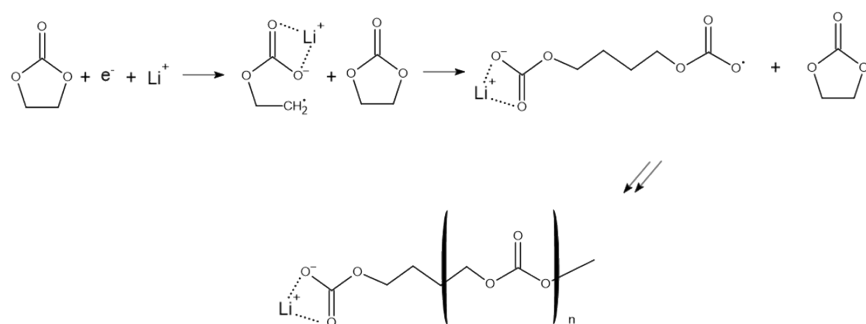


Fig. S3. Liquid chromatography mass spectrum of LiMPTFSI.

(a)



(b)

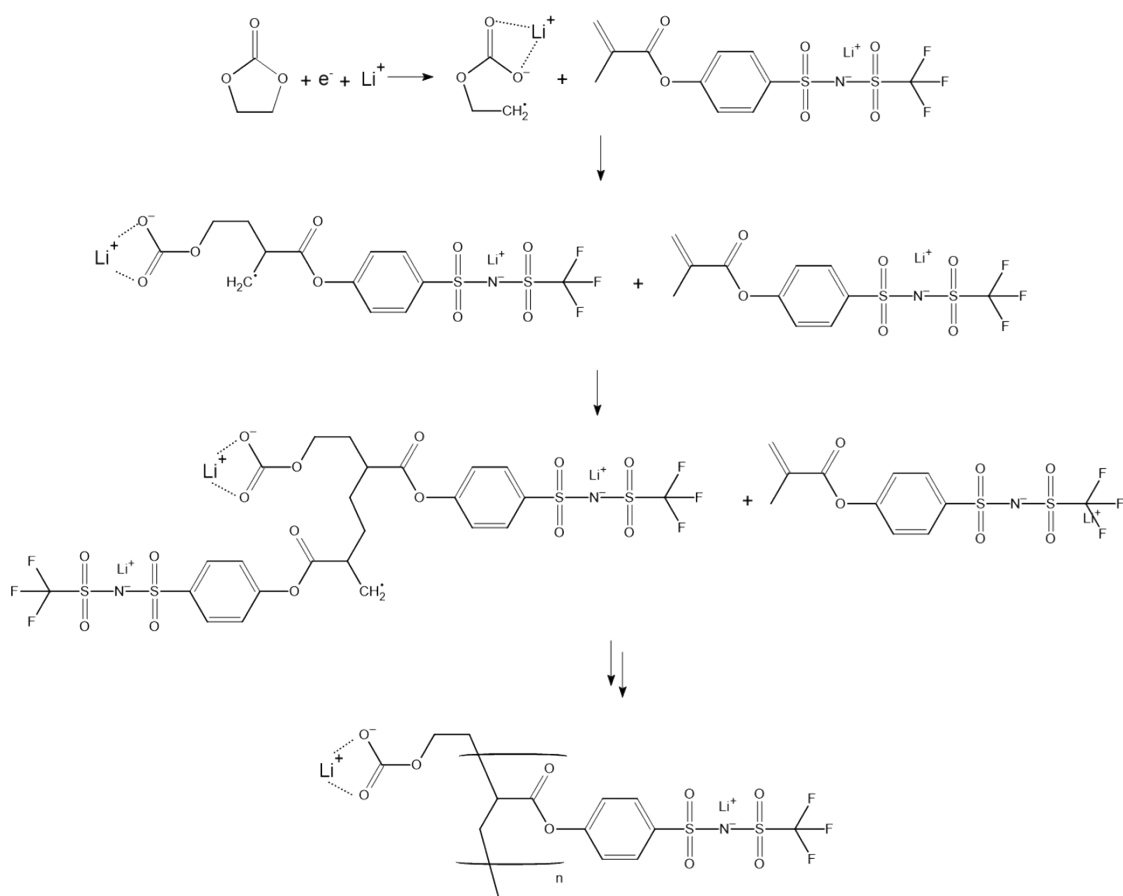


Fig. S4. Polymerization pathways of (a) EC and (b) LiMPTFSI by EC radical initiation.

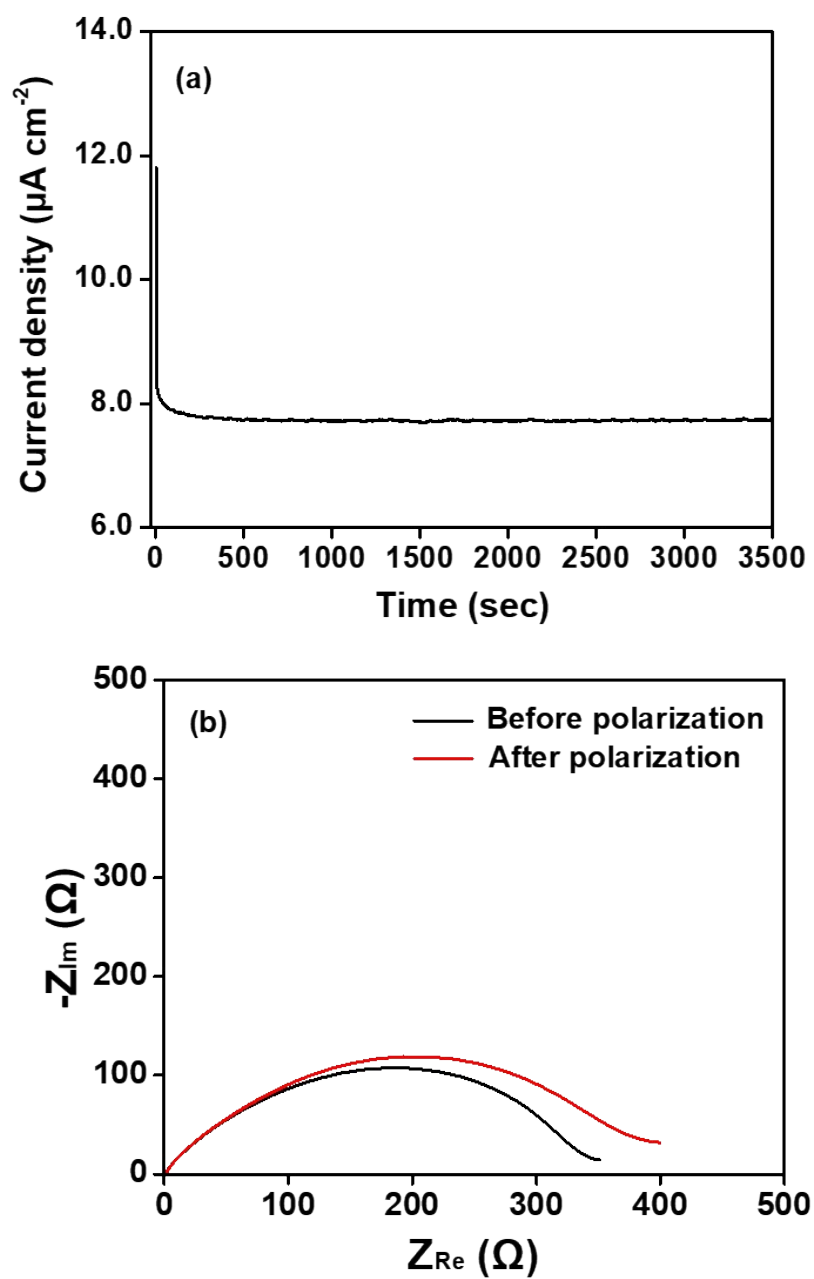


Fig. S5. (a) DC polarization curve and (b) AC impedance spectra of the surface-modified Li symmetric cell with the base electrolyte.

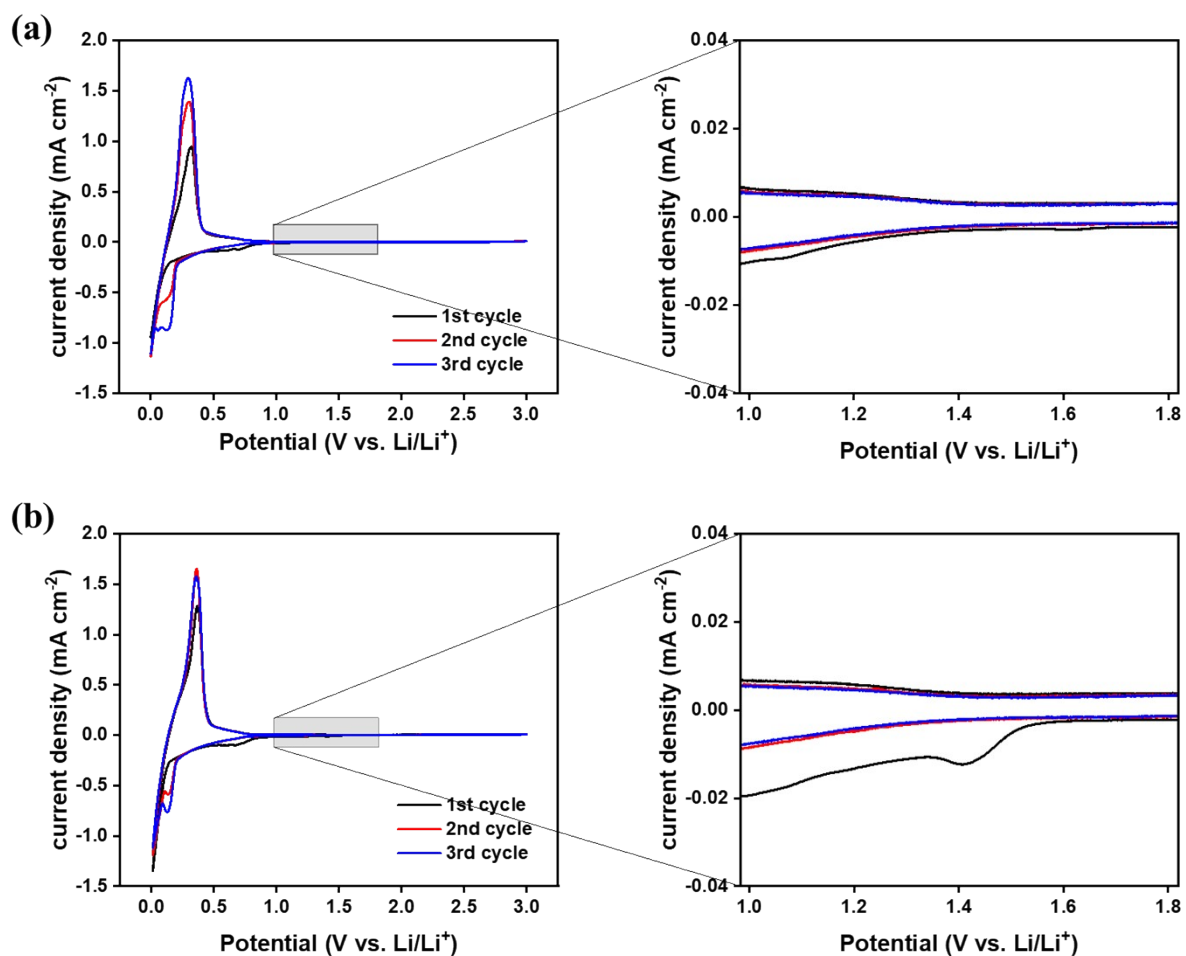


Fig. S6. Cyclic voltammograms of Li/graphite half-cells using a base electrolyte (a) without and (b) with 0.5 wt.% LiMPTFSI.

Table S1. The values of R_b , R_{SEI} , and R_{ct} in the cells with different electrolytes.

| Electrolyte | R_b (Ω) | R_{SEI} (Ω) | R_{ct} (Ω) |
|------------------------|--------------------|------------------------|-----------------------|
| Base electrolyte | 2.86 | 3.32 | 12.11 |
| With 0.5 wt.% LiMPTFSI | 2.66 | 4.83 | 8.33 |

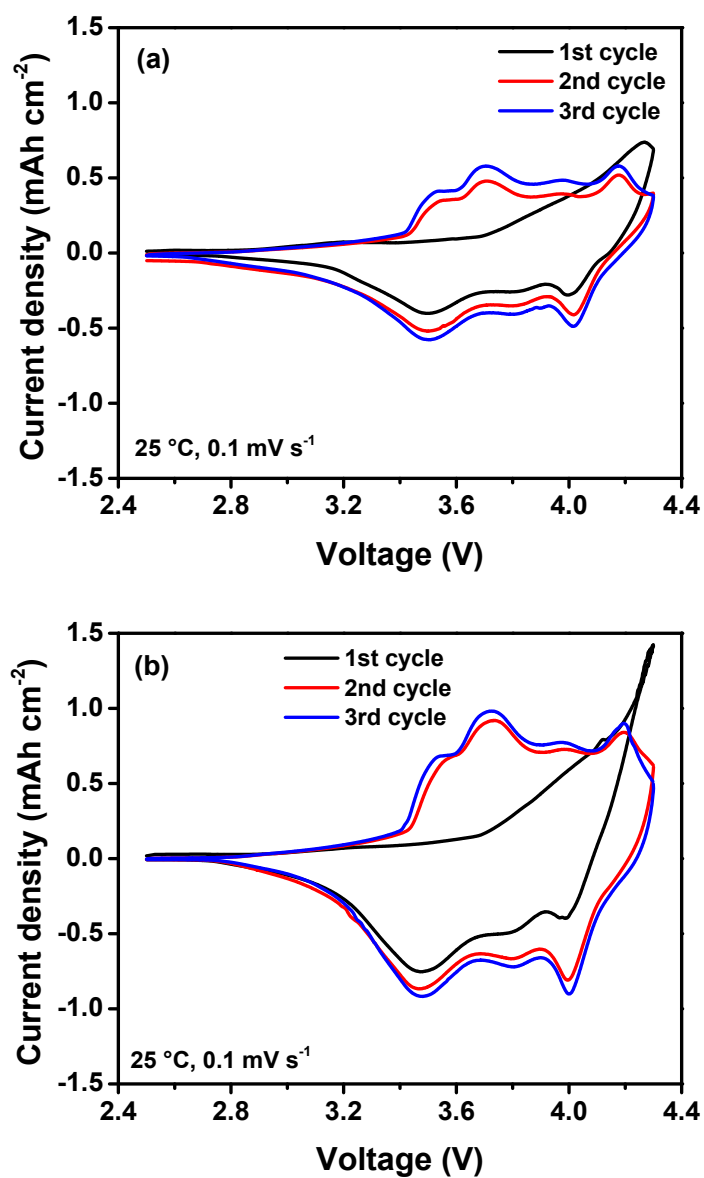


Fig. S7. CV curves of graphite/NCM full cells using base electrolyte (a) without and (b) with 0.5 wt.% LiMPTFSI.

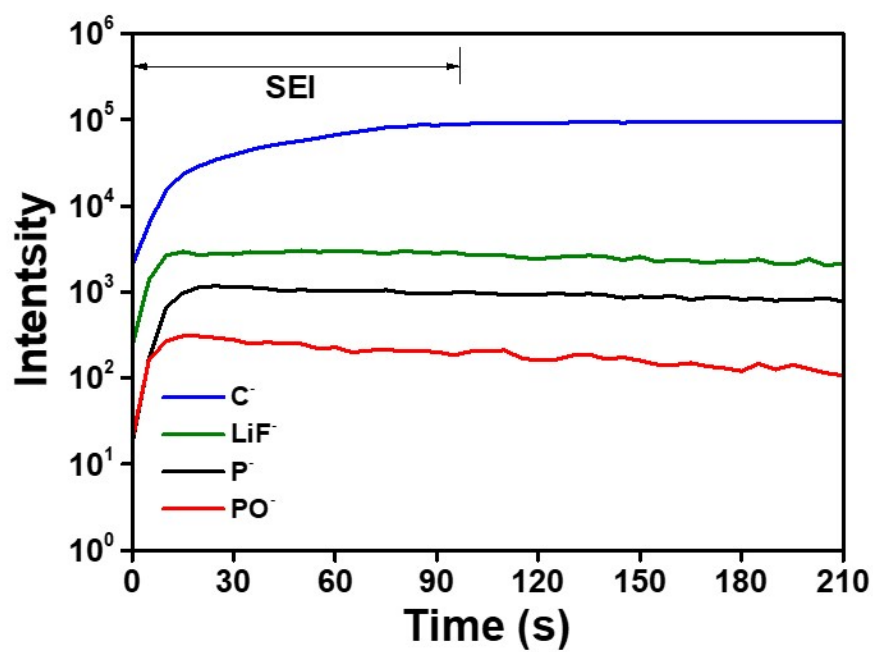


Fig. S8. ToF-SIMS depth profiles of a graphite anode with a base electrolyte after pre-cycling.

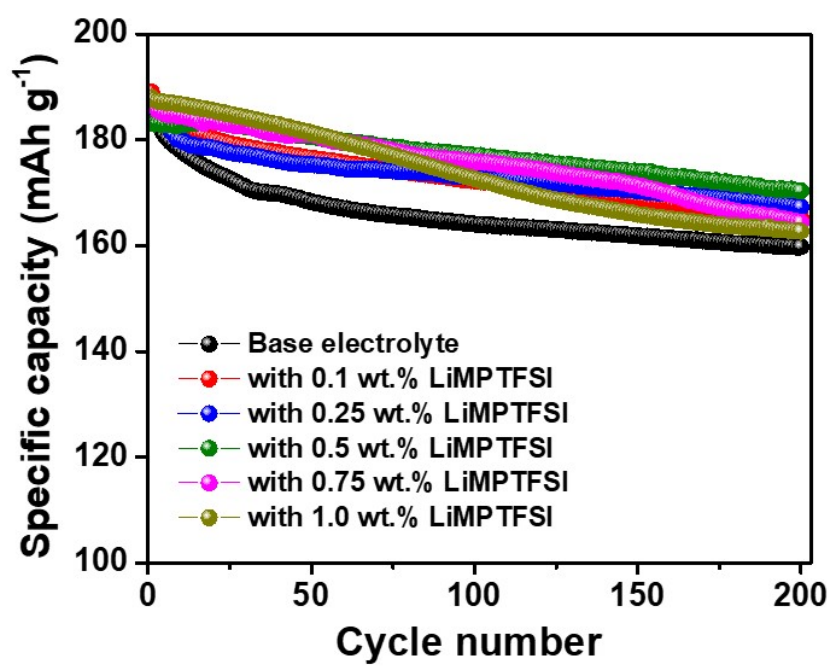
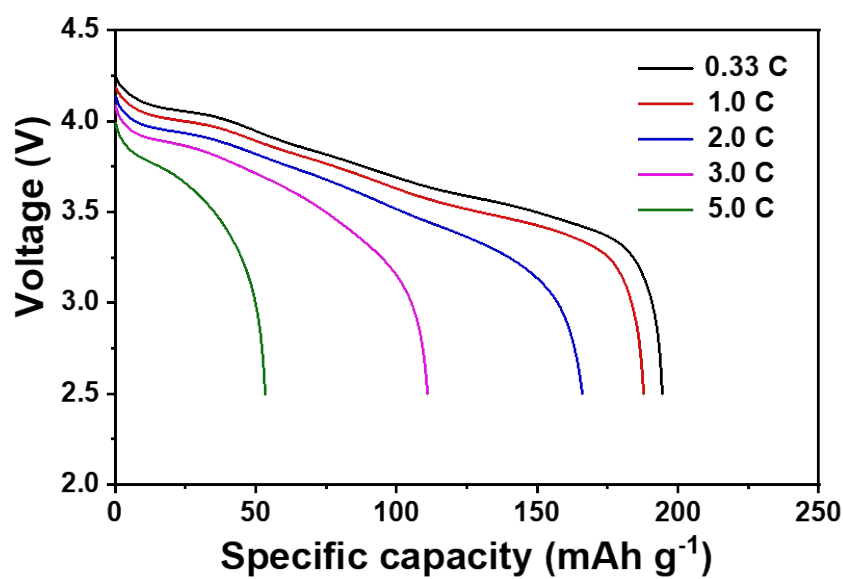


Fig. S9. Cycling performance of the Gr/NCM full cells with liquid electrolytes containing different amounts of LiMPTFSI at 1.0 C rate and 25 °C.

(a)



(b)

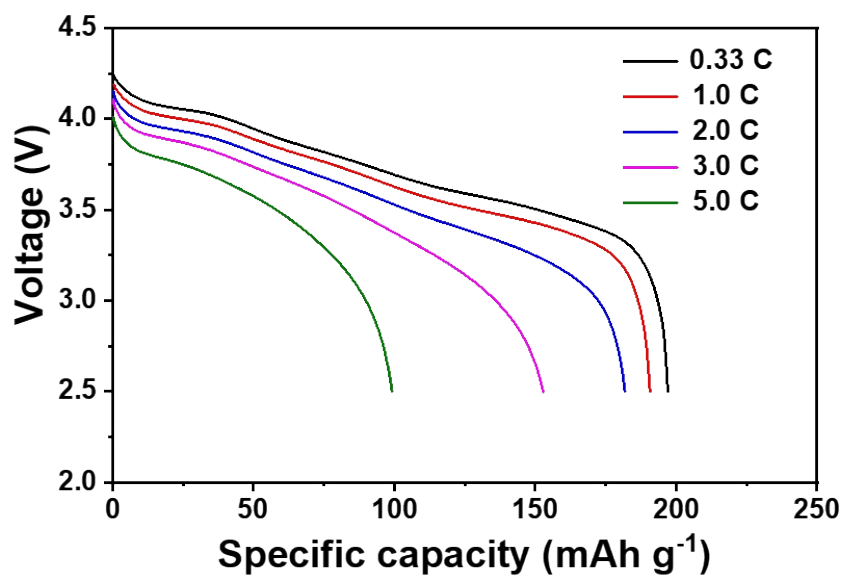


Fig. S10. Discharge curves of the Gr/NCM full cells using a base electrolyte (a) without and (b) with 0.5 wt.% LiMPTFSI at different C rates.

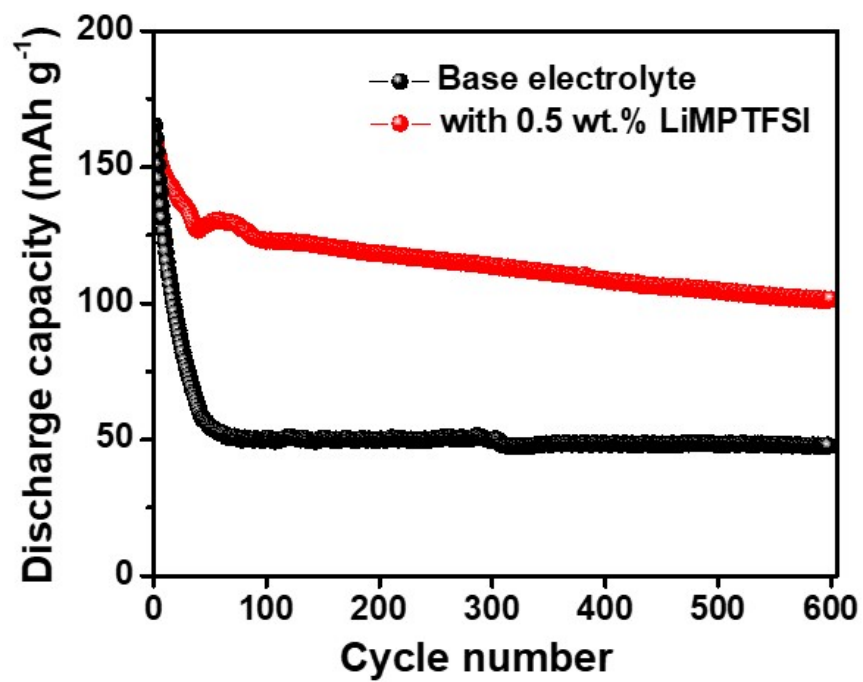


Fig. S11. Cycling performance of the Gr/NCM full cells using a base electrolyte with and without 0.5 wt.% LiMPTFSI at 2.0 C rate and 25 °C.

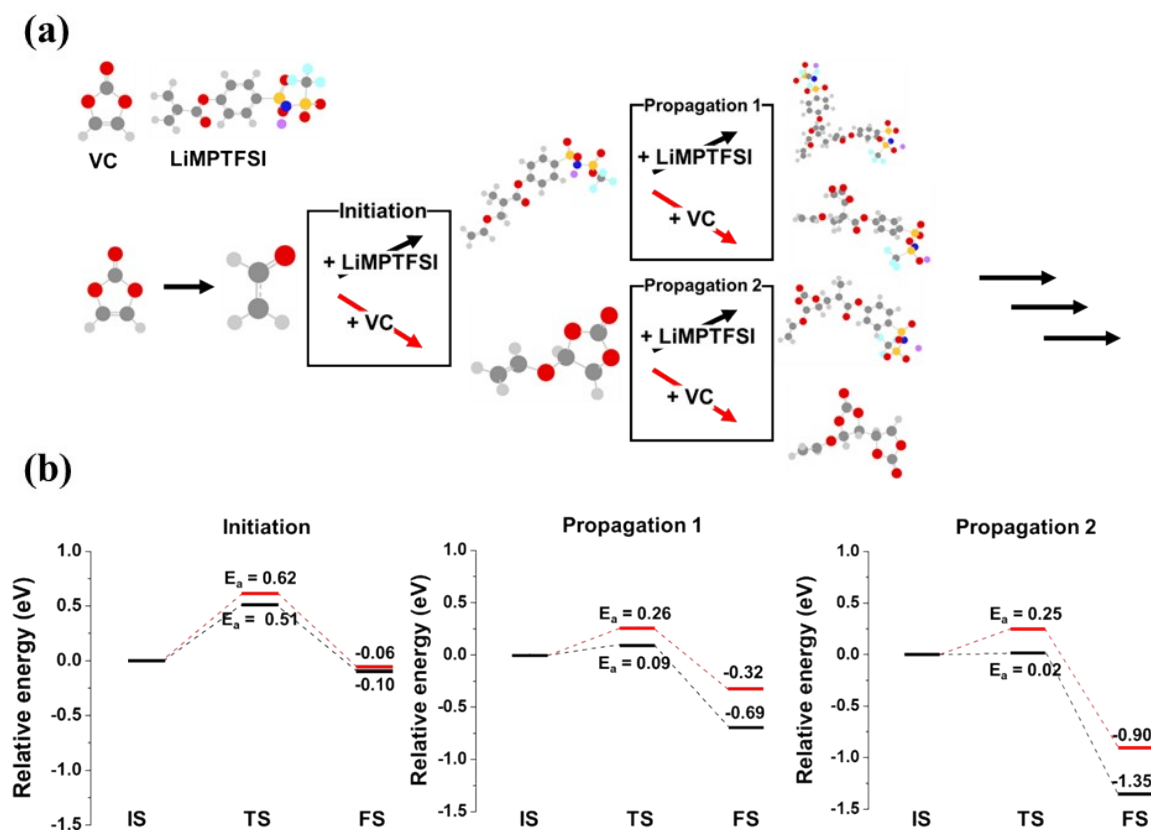


Fig. S12. (a) Schematic illustration and (b) relative energy diagram for polymerization of VC with another VC or LiMPTFSI. IS, TS, and FS denote initial state, transition state, and final state, respectively.

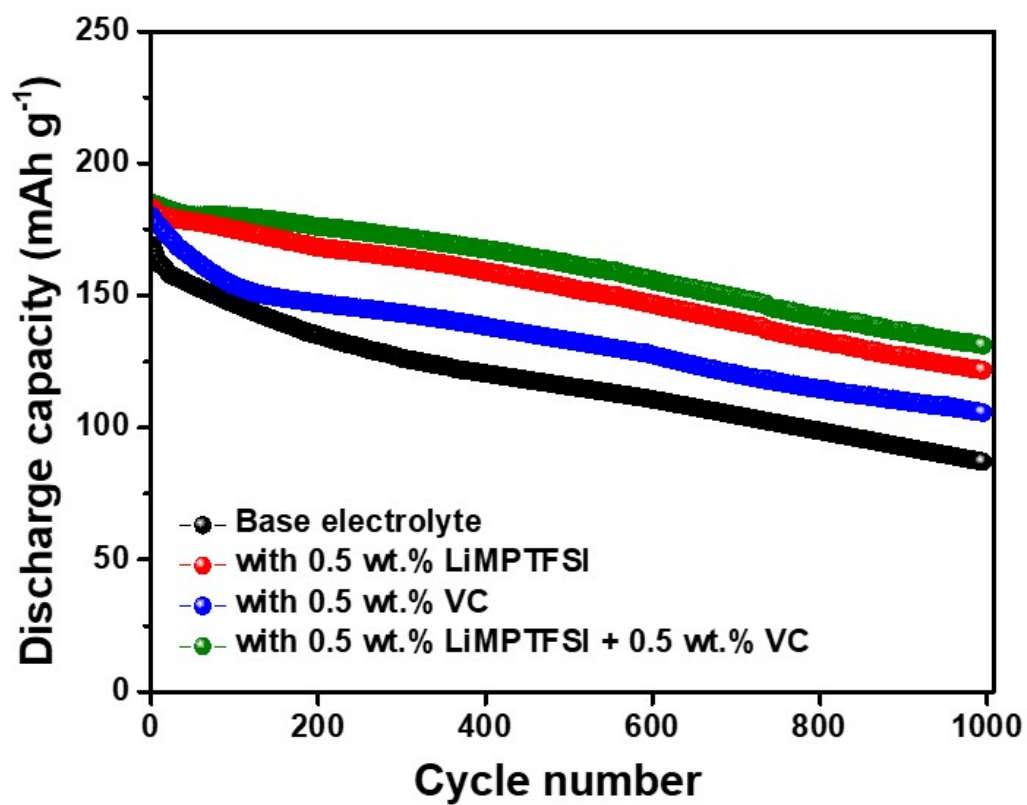


Fig. S13. Cycling performance of the Gr/NCM full cells using a liquid electrolyte containing different types of additives at a rate of 1.0 C.

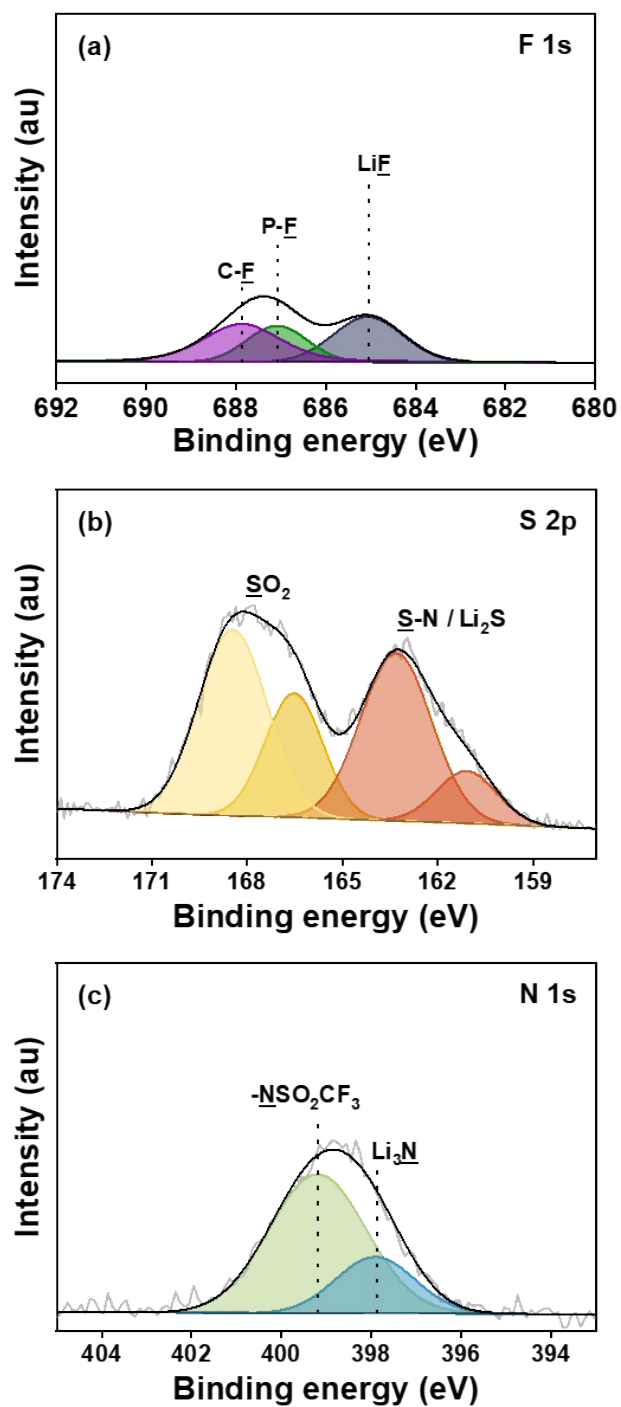


Fig. S14. (a) F 1s, (b) S 2p and (c) N 1s XPS spectra of the surface of the graphite anode cycled in a base electrolyte containing 0.5 wt.% LiMPTFSI after pre-cycling.

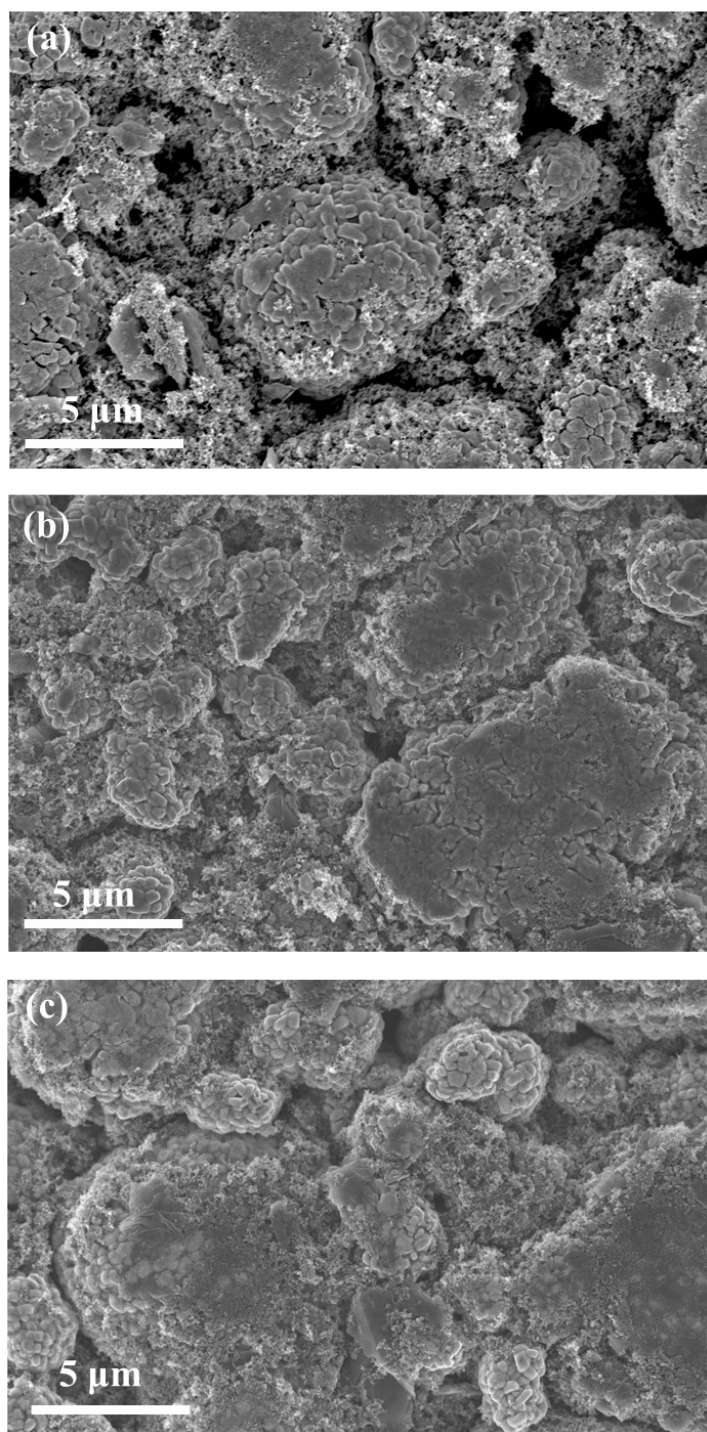


Fig. S15. SEM images of (a) pristine NCM cathode and NCM cathodes after the 500th cycle in a (b) base electrolyte and (c) with 0.5 wt.% LiMPTFSI.

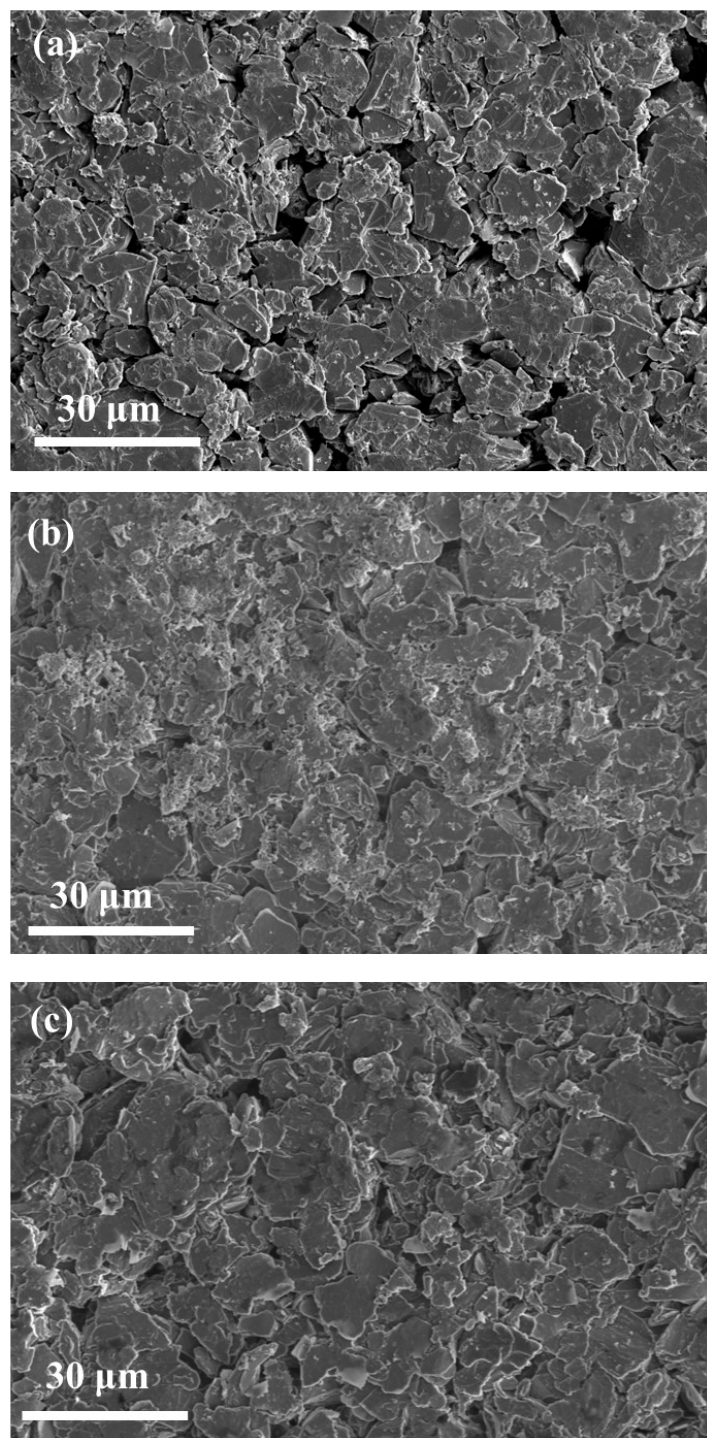


Fig. S16. SEM images of (a) a pristine graphite anode and graphite anodes after the 500th cycle in a (b) base electrolyte and (c) with 0.5 wt.% LiMPTFSI.

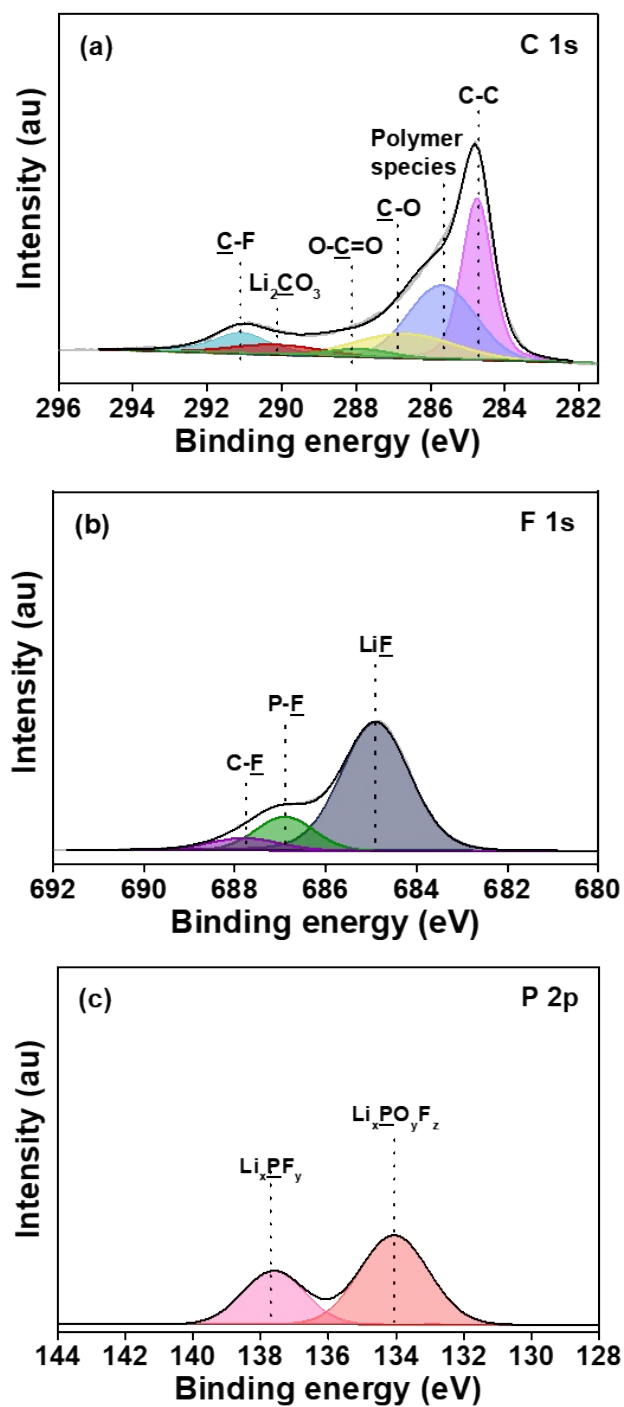


Fig. S17. (a) C 1s, (b) F 1s and (c) P 2p XPS spectra of the surface of the graphite anode after pre-cycling using a base electrolyte.

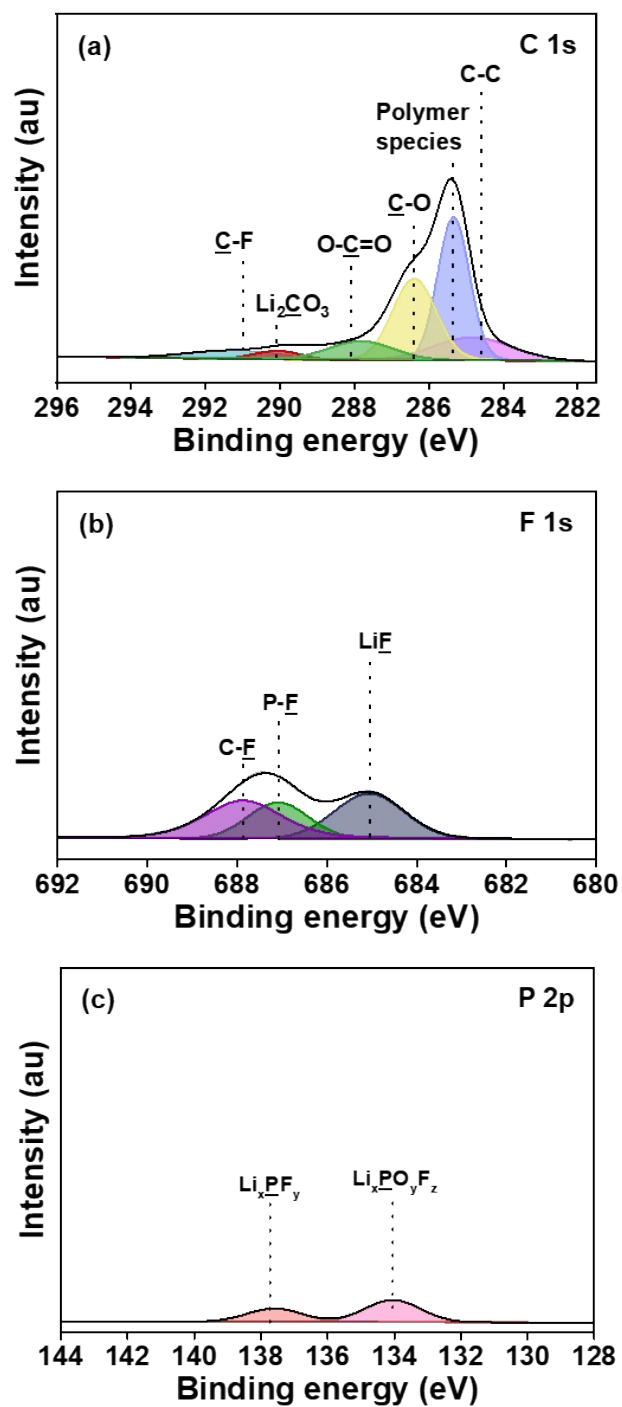


Fig. S18. (a) C 1s, (b) F 1s and (c) P 2p XPS spectra of the surface of a graphite anode after pre-cycling using a base electrolyte with 0.5 wt.% LiMPTFSI.